

AMBER/VLTI observations of 5 giant stars [★]

F. Cusano^{1,2}, C. Paladini³, A. Richichi^{4,5}, E. W. Guenther², B. Aringer⁶,
K. Biazzo¹, R. Molinaro¹, L. Pasquini⁵, and A. P. Hatzes²

¹ INAF-Osservatorio Astronomico di Capodimonte, Salita Moiariello16, I - 80131 Napoli, Italy ^{**}

² Thüringer Landessternwarte Tautenburg, Sternwarte 5, D - 07778 Tautenburg, Germany

³ Institut für Astronomie der Universität Wien, Türkenschanzstrae 17, A-1180 Wien, Österreich

⁴ National Astronomical Research Institute of Thailand, 191 Siriphanich Bldg., Huay Kaew Rd., Suthep, Muang Chiang Mai 50200 Thailand

⁵ European Southern Observatory, Karl-Schwarzschildstr. 2, D-85748 Garching bei München, Germany

⁶ INAF-Osservatorio Astronomico di Padova, Vicolo dell'Osservatorio 5, I - 35122 Padova, Italy

Received; accepted

ABSTRACT

Context. While the search for exoplanets around main sequence stars more massive than the Sun have found relatively few such objects, surveys performed around giant stars have led to the discovery of more than 30 new exoplanets. The interest in studying planet hosting giant stars resides in the possibility of investigating planet formation around stars more massive than the Sun. Masses of isolated giant stars up to now were only estimated from evolutionary tracks, which led to different results depending on the physics considered. To calibrate the theory, it is therefore important to measure a large number of giant star diameters and masses as much as possible independent of physical models.

Aims. We aim in the determination of diameters and effective temperatures of 5 giant stars, one of which is known to host a planet. We used optical long baseline interferometry with the aim of testing and constraining the theoretical models of giant stars. Future time-series spectroscopic observations of the same stars will allow the determination of masses by combining the asteroseismological analysis and the interferometric diameter.

Methods. AMBER/VLTI observations with the ATs were executed in low resolution mode on 5 giant stars. In order to measure high accurate calibrated squared visibilities, a calibrator-star-calibrator observational sequence was performed.

Results. We measured the uniform disk and limb-darkened angular diameters of 4 giant stars. The effective temperatures were also derived by combining the bolometric luminosities and the interferometric diameters. Lower effective temperatures were found when compared to spectroscopic measurements. The giant star HD12438 was found to have an unknown companion star at an angular separation of ~ 12 mas. Radial velocity measurements present in the literature confirm the presence of a companion with a very long orbital period ($P \sim 11.4$ years).

Key words. giant stars – exo-planet – interferometry – fundamental parameters

1. Introduction

The relation between the mass of hosting stars and planets has been investigated theoretically by several authors (Kornet et al. 2006; Kennedy & Kenyon 2008; Raymond et al. 2007). According to these works there is a dependence between the frequency of giant planets and the mass of the hosting star. Radial velocity (RV) surveys clearly demonstrate that the frequency of Jupiter-mass planets around M-type stars is much lower than that of the more massive solar-like stars (Endl et al. 2006; Johnson et al. 2007). Unfortunately, probing this relation for stars more massive than the Sun, from an observational point of view, is quite difficult due to the limitations in detecting planets around high mass stars. Main sequence stars more massive than the Sun show few and broad spectral lines, due to the higher effective temperatures, gravity, and rotation. Detecting planets around these stars using the RV technique is very challenging, and up to now only few planets have been discovered (e. g., Guenther et al. 2009; Hartmann et al. 2010). The search for exoplanets can be indeed performed on giant stars, which have more

and sharper absorption lines respect to main sequence stars of similar masses, due to cooler photospheres, lower gravity, and slower rotation rate. Up to now, 31 exoplanets are known orbiting giant stars (see Planet Encyclopaedia¹) and certainly this number is destined to increase in the near future thanks to the ongoing observational campaigns. In order to study the relation between the mass of the planet and the parent star, it is of fundamental importance to determine as accurately as possible the mass of the star. Currently, masses of isolated giant stars are only determined by comparison with evolutionary models. Although in the recent years the stellar evolutionary calculations have reached a highly sophisticated level, there is still no convergence among the authors on the treatment of input physics such as opacity and metallicity. This can lead to different mass estimations for the same object. Therefore it is of fundamental importance to calibrate the theoretical models, measuring physical parameters of a certain number of giant stars, using model independent techniques.

It is well established that giant stars show solar like pulsations, with typical periods longer than that of main sequence stars (Hekker et al. 2009; Kallinger et al. 2010; Bedding et al.

^{*} Based on observations carried out at the European Southern Observatory (Paranal, Chile) under programme No. 082.D-0337.

^{**} email: fcusano@na.astro.it

¹ <http://www.exoplanet.eu>

2010). The asteroseismological analysis of pulsating stars allows one to derive the average density of a star, through the determination of the primary frequency splitting $\Delta\nu$ (i. e. the frequency difference between two harmonic modes characterized by different consecutive radial order n and same angular degree l ; Kjeldsen & Bedding 1995). Combining this measure with the radius obtained using optical long baseline interferometry, it is then possible to derive the mass of the star. This technique has been successfully applied to the subgiant star β Hyi by North et al. (2007), where the mass was determined with an error $< 3\%$. Hatzes & Zechmeister (2007) used RV measurements of the stellar oscillations in the planet hosting stars giant star β Gem combined with the interferometrically measured stellar radius to confirm that the star had a mass of $\approx 2 M_{\odot}$. The frequency of maximum amplitude oscillations ν_{max} is also related to the mass of the star, via the radius and the temperature (see Kjeldsen & Bedding 1995). The detection of this frequency is less observationally time consuming and gives also a good estimate of the mass. In principle, the mass and radius can be derived from a knowledge of $\Delta\nu$ and ν_{max} , but this is still not as accurate as using additional information on the stellar radius. Unlike main sequence stars, giant stars of similar effective temperatures have a wide range of radii (10–60 R_{\odot}). An error of 20% in the radius corresponds to an error of 60% in the stellar mass, which is crucial for planet formation theory. Thus asteroseismology alone, via the spacing of p -modes, does not provide the mass of a star with the accuracy needed (see Kjeldsen & Bedding 1995).

It is therefore essential to obtain good measurements of the angular diameter as an accurate stellar radius is required by asteroseismic studies. If one invests large amounts of telescope time to derive the oscillation spectrum, and then optical long baseline interferometry is unable to determine the radius (e.g. unresolved source), then the asteroseismic data will be of a limited use. After a large number of giant star diameters will be measured using interferometers, such as the VLTI (Very Large Telescope Interferometer; Hagenauer et al. 2008), then asteroseismological observational campaigns can be performed on the most interesting targets.

This paper is organized as follow: in Sect. 2 the observations and the data reduction are presented; the determination of angular diameter and effective temperature by the UD-fit and LD-fit is presented in Sect. 3; Section 4 reports the discovery of the binary HD12438; results and conclusions are presented in Sect. 5.

2. Observations and data reduction

2.1. Description

Our project started by observing interferometrically five giant stars with AMBER, which is the near infrared VLTI instrument that combines the light from three different telescopes (Petrov et al. 2007). AMBER was used in combination with the Auxiliary Telescopes (ATs) adopting the telescope stations A0-K0-G1. The configuration of the telescopes is triangular, with two almost identical baselines of 90.5 m (G1-K0 and A0-G1), and one of 128 m (A0-K0). Observations were performed in LR-mode ($R=35$) for a total of 20 hours spread over 9 different nights in the period between October and December 2008. A summary of the observations is presented in Table 1. The targets chosen are listed in Table 2, together with some parameters from the literature. The five stars were selected from the da Silva et al. (2006) sample and were chosen in order to cover a wide range of metallicities, predicted masses, and radii. This will allow us to

test theoretical models in different conditions. One of these stars, namely HD11977, is known to host a planet orbiting the star with a period of 711 days (Setiawan et al. 2005). The predicted variability of these giant stars due to solar-like oscillations does not effect the interferometric observations, because the radius variations due to the restoring of the p force are just of few kilometers at most. Additional sources of variability that could alter the interferometric observations are not known for our target stars.

2.2. Observation and data reduction

In order to have reliable data, AMBER was used in combination with the fringe tracker. FINITO is the VLTI fringe-tracker whose purpose is to compensate the atmospheric turbulence effect on two telescopes and to introduce an additional difference in the optical difference path (Le Bouquin et al. 2008). FINITO was used to track the fringes for all the objects except HD12438 that was too faint. A detector integration time (DIT) of 50 ms was used for each frame. Every exposure consists of a cube of 1000 frames. Five exposures were acquired for each observation of a scientific (calibrator) star. In order to obtain accurate measurements of the squared visibility, the observational sequence calibrator-star-calibrator (CAL-SCI-CAL) was adopted. This means that a calibrator star was observed shortly before and after the scientific target. The calibrator stars were chosen to be nearby ($< 10^{\circ}$), and within a range of ± 0.5 mag in the K band with respect to the scientific target. The 9 calibrators (one calibrator star, HD24150, was used for two scientific targets) presented in Table 3 were selected using the web-interface *CalVin*². For each observational sequence, 1.50 hours were needed, including the internal calibration.

The data reduction was performed using the software *Amdlib*³ provided by the Jean-Marie Mariotti Center. Details of the AMBER data reduction are explained in Tatulli et al. (2007) and Chelli et al. (2009). In order to obtain the squared visibilities for each exposure, we averaged the frames after a frame selection. The selection was performed keeping 20% of the frames with the highest signal-to-noise ratio (S/N). This criterion was applied for both the calibrators and the science targets.

2.3. Visibility calibration

The command line *amdlibDivide* in *Amdlib* was used to derive the calibrated squared visibility for each scientific exposure. This command line derives calibrated visibility of the science targets using the following relationship:

$$V_{\text{calS}}^2 = \frac{V_{\text{obsS}}^2}{V_{\text{obsC}}^2/V_{\text{teoC}}^2} \quad (1)$$

where V_{calS}^2 is the calibrated squared visibility of the science target, V_{obsS}^2 is the observed squared visibility of the science target, V_{obsC}^2 is the observed squared visibility of the calibrator star and V_{teoC}^2 the expected visibility of the calibrator star. Each scientific exposure was calibrated with each exposure of the two corresponding calibrators. The calibrated squared visibilities were then averaged. This procedure was performed for each observing block. Fig. 1 shows an example of the squared visibilities of HD12438 (Obs. 5 Oct 2008) calibrated with HD19869 (dot symbols) and HD10537 (cross symbols). In order to make the plot

² <http://www.eso.org/observing/etc/>

³ http://www.jmmc.fr/data_processing_amber.htm

Table 1. Observing log. All the observations were performed during the year 2008, using the ATs station A0-G1-K0, DIT=50 ms and a CAL-SCI-CAL sequence. In the last columns the average statistical error in the H and K bands are given in percentage.

Target	Calibrator	Obs. date	N	$\sigma_{\text{stat}}(H)(\%)$	$\sigma_{\text{stat}}(K)(\%)$
HD11977	HD5457, HD24150,	7 Oct	2	5.2	5.0
		22 Dec	1	6.1	6.0
HD12438	HD10537, HD16897	5 Oct	1	6.4	6.2
		6 Oct	2	5.3	5.2
		20 Dec	1	5.4	5.1
HD23319	HD22663, HD24150	7 Oct	1	3.3	3.5
		10 Dec	1	4.2	4.6
HD27256	HD27442, HD28413	21 Dec	1	6.4	6.1
		23 Dec	1	5.4	5.3
		24 Dec	2	5.4	5.1
		25 Dec	1	6.5	6.6
HD36848	HD33872, HD34642	21 Dec	1	7.2	7.1
		22 Dec	1	8.2	8.4

Table 2. Giant stars observed with AMBER.

ID	Ra (J2000)	Dec (J2000)	V (mag)	K (mag)	Sp. Type	π (mas)	[Fe/H] (dex)
HD11977	01 54 56	-67 38 50	4.70	2.590 \pm 0.240	G8.5 III	14.91 \pm 0.16	-0.21
HD12438	02 01 15	-30 00 07	5.35	3.218 \pm 0.298	G5 III	11.08 \pm 0.29	-0.61
HD23319	03 42 50	-37 18 49	4.60	2.639 \pm 0.274	K2.5 III	17.70 \pm 0.22	0.24
HD27256	04 14 25	-62 28 26	3.34	1.439 \pm 0.312	G8 II-III	20.18 \pm 0.10	0.07
HD36848	05 32 51	-38 30 48	5.46	2.804 \pm 0.268	K2 III	18.93 \pm 0.23	0.21

Note that the V magnitudes and the spectral types are taken from *Simbad*. The K magnitudes are from 2MASS (Skrutskie et al. 2006). The parallaxes are from the new reduction of Hipparcos data (van Leeuwen 2007). The metallicities are from da Silva et al. (2006).

more clear, the visibilities of the baselines B2 and B3 were arbitrarily shifted by -0.5 and $+0.5$, respectively. The final products are squared visibility measurements in H and K band spectral channels.

2.4. Error estimation

The final error on the calibrated squared visibility is given by two principal components: (i) a statistical error due to the dispersion of the visibility in between the single exposure; (ii) a systematic error defined by the uncertainty in the calibrator angular diameter. The statistical error was computed taking the standard deviation relative to the averaged calibrated visibilities. The robustness of the choice of the standard deviation was tested using a bootstrap method. We combined the calibrated visibilities of one OB of HD27256 by using a bootstrap analysis (Efron 1979). The resampling of the data was performed 500 times and the variance of the sample average was computed. This last resulted to be of the same order of the standard deviation for most of the data involved in the test. For this reason we kept the standard deviation of the average as the statistical error of the calibrated visibilities.

The effect of the calibrator angular diameter uncertainty on the calibrated visibility was computed analytically. The computation of this systematic error on the calibrated visibility was performed by using for each target star the corresponding calibrators adopting the error on the diameter given in Table 3. In the computations performed, we are also taken into account the wavelength range and the different baselines. The root mean square (rms) on the final calibrated-visibilitys is of $\sim 2.4\%$.

The average error performed in the measure of the calibrated visibilitys is of $\sim 8\%$. In the best case we obtained calibrated visibilitys with 5.5% of accuracy (for HD27256), while in the

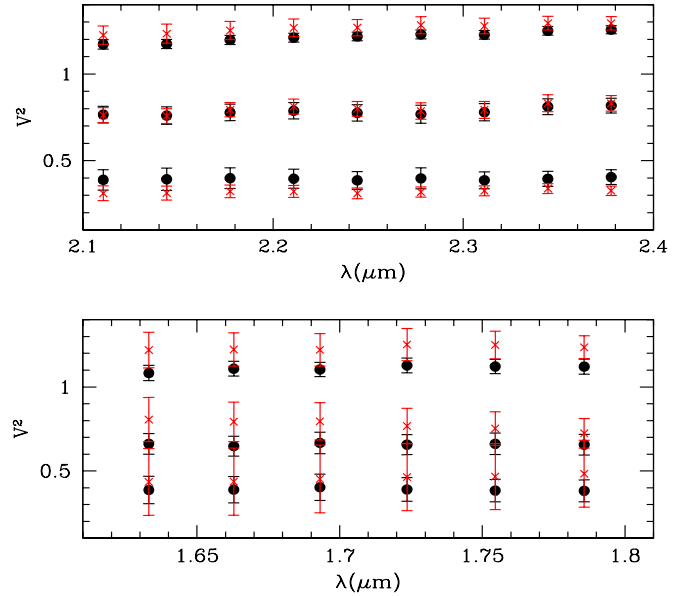


Fig. 1. Calibrated squared-visibilitys of HD12438. The black dots are the calibrated visibilitys using the calibrator HD16987, while the red crosses are those ones using the calibrator HD10537. More details are given in Sect. 2.3.

worst case (for the star HD36848) we had 11% accuracy in one observing block.

2.5. Closure phase

Together with the squared-visibility, another important observable that can be extracted by the AMBER data is the closure phase (CP). The CP allows one to improve the investigation of the shape of a target. For example, the CP of an object with a circular-symmetric distribution of the light is always zero. Reliable CP measurements for the five giant stars were derived by the AMBER data using the software *Amdlib*. These CPs were calibrated for instrumental effect by using the CPs measured for the calibrator stars. Further discussion on the CP are presented in Sect. 4.

3. Angular diameter and effective temperature determination

The first step of our analysis was to estimate the angular diameters of the target stars by fitting the AMBER data to a Uniform Disk (UD) analytical function. The UD is often used in the literature to approximate the size of a single star (e. g., Dyck et al. 1998). This approach can be very misleading for extended atmospheres (Jacob & Scholz 2002; Paladini et al. 2009), while it gives reasonable results in case of objects with an almost hydrostatic atmosphere, like K-giants.

The angular diameters were derived fitting the squared-visibility measured with AMBER to the model of a UD star:

$$V^2(\theta_{UD}) = \left[\frac{2J_1\left(\frac{\pi B \theta_{UD}}{\lambda}\right)}{\frac{\pi B \theta_{UD}}{\lambda}} \right]^2 \quad (2)$$

where J_1 is the Bessel function of the first order, B is the projected baseline and θ is the stellar angular diameter. An example of the UD fit is shown in Fig. 2. Angular diameters of the scientific targets were derived by the UD-fit for each spectral channels in the H and K bands. The errors are calculated by deriving the diameter at $\chi^2_{min} + 1$ on both sides of the minimum χ^2 and determining the difference between the χ^2_{min} diameter and $\chi^2_{min} + 1$ diameter. We thus computed the averaged diameters in the H and K bands, using the values derived in the spectral range 1.6-1.8 μm for the H band and 2.1-2.4 μm for the K band. The errors on the averaged H and K diameters were derived adding the average error of the diameters calculated in the single spectral channel to the standard deviation. The UD angular diameters are listed in Table 4.

The limb-darkened diameters (LD) were obtained by fitting the data to equation (Hanbury Brown et al. 1974):

$$V^2(\theta_{LD}) = \left(\frac{1 - \mu_\lambda}{2} + \frac{\mu_\lambda}{3} \right)^{-1} \quad (3)$$

$$\times \left[(1 - \mu_\lambda) \frac{J_1\left(\frac{\pi B \theta_{LD}}{\lambda}\right)}{\frac{\pi B \theta_{LD}}{\lambda}} + \mu_\lambda \left(\frac{\pi}{2} \right)^{1/2} + \frac{J_{3/2}\left(\frac{\pi B \theta_{LD}}{\lambda}\right)}{\left(\frac{\pi B \theta_{LD}}{\lambda}\right)^{3/2}} \right]$$

with μ_λ the linear LD coefficient. The latter was obtained from Claret et al. (1995) adopting the T_{eff} and $\log g$ values from da Silva et al. (2006). The errors on the LD angular diameters were derived as explained above for the UD angular diameters. The LD angular diameters derived are listed in Table 4, together with linear radii. These lasts were calculated using the average LD diameters and the parallaxes taken from van Leeuwen (2007).

Table 3. Calibrator star informations. The parameters are taken from the catalogs Mérand et al. (2005) and Bordé et al. (2002).

Star	V (mag)	K (mag)	Sp. Type	$\theta_{UD} (H)$ (mas)	$\theta_{UD} (K)$ (mas)
HD5457	5.46	2.98	K2III	1.29 ± 0.02	1.29 ± 0.02
HD24150	6.76	2.56	K5/M0III	1.53 ± 0.02	1.55 ± 0.02
HD10537	5.26	2.95	K0III	1.29 ± 0.02	1.30 ± 0.02
HD16897	7.40	2.97	M0III	1.27 ± 0.02	1.28 ± 0.02
HD22663	4.59	2.04	K1III	1.89 ± 0.02	1.90 ± 0.02
HD27442	4.44	1.75	K2IVa	1.89 ± 0.05	1.90 ± 0.05
HD28413	5.95	2.41	K4.5III	1.85 ± 0.05	1.87 ± 0.05
HD33872	6.59	2.28	K5III	1.86 ± 0.03	1.88 ± 0.03
HD34642	4.83	2.67	K0IV	1.49 ± 0.02	1.50 ± 0.02

Once the θ_{LD} were determined interferometrically, the effective temperatures T_{eff} were calculated by using the relationship:

$$T_{\text{eff}} = \left(\frac{4F_{\text{bol}}}{\theta_{LD}^2 \sigma} \right)^{1/4} \quad (4)$$

where F_{bol} is the bolometric flux and σ is the Stefan-Boltzmann constant. The average of the H and K band LD angular diameters was used in Eq. 4. The bolometric flux was calculated by applying the bolometric corrections from Pickles (1998) to the de-reddened V magnitude. The A_V for each star was derived by the $E(V-K)$ using the extinction curve reported by Cardelli et al. (1989). The $E(V-K)$ was calculated from the observed $(V-K)$ and the intrinsic $(V-K)_0$ using the spectral type reported in Table 2 and the conversion table of Pickles (1998). The final effective temperatures are presented in Table 4.

4. Binary discovery: HD12438

We were able to fit the angular diameters in each spectral channel with $< 5.5\%$ accuracy for all the stars, with the exception of HD12438. The quality of the data for this star was the same as for the other scientific targets. We speculated at this point that this star could have a companion; in fact a single star model was not able to reproduce the visibilities. A clue in this direction was given by the fact that the measured visibilities on the baselines G1-K0 and A0-G1, that have almost the same length, but different orientation, were different. In order to confirm our hypothesis we developed at this point a software to fit the observed visibilities to a model of a pair of resolved stars. HD12438 was observed 4 times with AMBER (see Table 1). More precisely, one observation was performed on the 5th of October, two on the 6th of October and one on the 20th of December, in 2008. The software calculates the angular separation between the components of the binary, the position angle, the flux ratio, and the angular diameters of the two components. The squared visibilities in this case are given by the equation:

$$V^2 = \frac{J_1(\theta_1) + J_2(\theta_2)f^2 + 2J_1(\theta_1)J_2(\theta_2)f \cos(2\pi \frac{\mathbf{B} \cdot \boldsymbol{\rho}}{\lambda})}{(1+f)^2} \quad (5)$$

where f is the flux ratio, J_1 and J_2 are the Bessel functions corresponding to the single binary components with angular diameters θ_1 and θ_2 , \mathbf{B} is the baseline vector, and $\boldsymbol{\rho}$ is the separation vector. The whole set of data of this star fits to the Eq. 5 better than to the relationship valid of a single star with an UD. Fitting the observed visibilities acquired at four different epochs to the Eq. 5, we estimated the separation angle between the components, which is $\rho = 12.0 \pm 4.0$ mas. The position angle of the

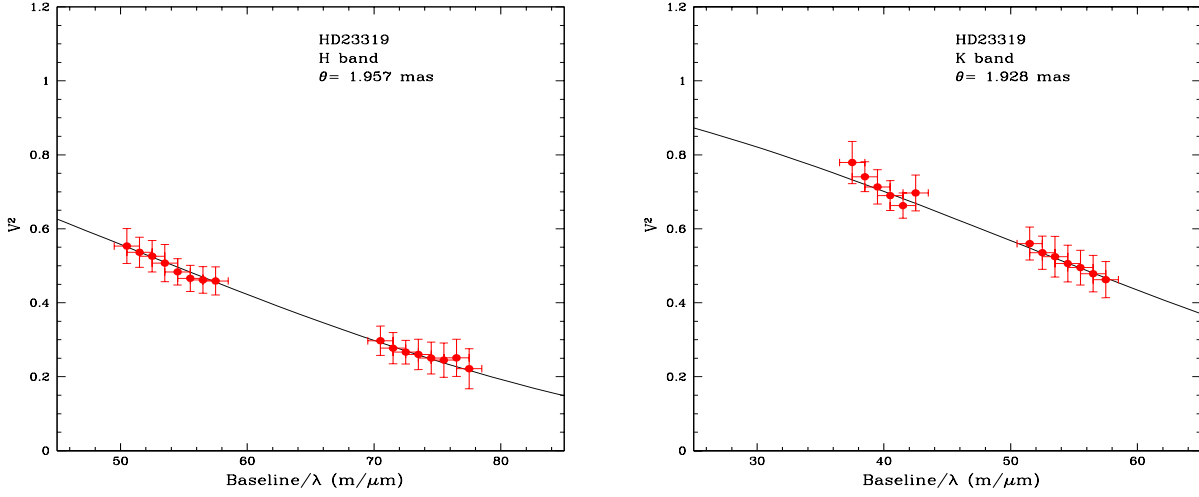


Fig. 2. AMBER observed visibilities in the H (left) and K band (right) for HD23319. The line represent the UD model (cfr. Eq. 2) computed with best fitting angular diameters to the corresponding band.

Table 4. Diameters measured with AMBER for the five giants.

ID	$\theta_{UD}(H)$ (mas)	$\theta_{UD}(K)$ (mas)	$\theta_{LD}(H)$ (mas)	$\theta_{LD}(K)$ (mas)
HD11977	$1.564 \pm 0.074^{stat} \pm 0.024^{syst}$	$1.573 \pm 0.048^{stat} \pm 0.033^{syst}$	$1.576 \pm 0.075^{stat} \pm 0.025^{syst}$	$1.580 \pm 0.048^{stat} \pm 0.033^{syst}$
HD12438*	1.0 ± 0.1	1.0 ± 0.1		
HD23319	$1.957 \pm 0.026^{stat} \pm 0.020^{syst}$	$1.928 \pm 0.044^{stat} \pm 0.029^{syst}$	$2.026 \pm 0.028^{stat} \pm 0.021^{syst}$	$1.982 \pm 0.046^{stat} \pm 0.028^{syst}$
HD27256	$2.559 \pm 0.025^{stat} \pm 0.065^{syst}$	$2.557 \pm 0.028^{stat} \pm 0.071^{syst}$	$2.639 \pm 0.027^{stat} \pm 0.071^{syst}$	$2.618 \pm 0.029^{stat} \pm 0.072^{syst}$
HD36848	$1.320 \pm 0.087^{stat} \pm 0.018^{syst}$	$1.350 \pm 0.093^{stat} \pm 0.025^{syst}$	$1.363 \pm 0.090^{stat} \pm 0.019^{syst}$	$1.386 \pm 0.095^{stat} \pm 0.026^{syst}$

*Note that for HD12438 we give the angular diameter of the primary, obtained by fitting the model of a resolved binary, as explained in the text.

Table 5. The linear radii and luminosities are derived by using the Hipparcos parallaxes reported in Table 2.

ID	R_{linear} (R_{\odot})	L (L_{\odot})	T_{eff} (K)
HD11977	$11.38 \pm 0.65^{stat} \pm 0.32^{syst}$	45.3 ± 8.4	4445 ± 125
HD12438	9.71 ± 1.34	48.0 ± 19.3	4884 ± 250
HD23319	$12.18 \pm 0.36^{stat} \pm 0.26^{syst}$	45.2 ± 4.5	4294 ± 58
HD27256	$14.01 \pm 0.22^{stat} \pm 0.54^{syst}$	91.6 ± 5.8	4777 ± 36
HD36848	$7.81 \pm 0.75^{stat} \pm 0.20^{syst}$	17.4 ± 5.1	4223 ± 209

angular separation is barely changing for observations separated by 2.5 months (6 October - 20 December 2008), indicating a long orbital period. The position angle has an average value of $120^{\circ} \pm 20^{\circ}$.

The primary star is resolved with the baselines chosen. The angular diameters of the primary and secondary are respectively of 1.0 ± 0.1 mas and ≤ 0.3 mas. The flux ratio ratio is ~ 0.028 both in the *H* and *K* bands. The calibrated closure phase also indicated that the object is not centro-symmetric, as it is different from zero to certain wavelengths. The comparison with the closure phases of the other 4 giant stars, presented in Fig. 3, clearly shows that HD12438 is not a single star.

Further confidence of the binarity of this object was given by the spectroscopy present in the literature. HD12438 was investigated spectroscopically as a part of planet search programs by Setiawan et al. (2004) and Hatzes (private communication) using the FEROS@ESO and HARPS@ESO spectrographs, respectively. The former observed this object for 5 years obtaining 61 spectra and finding a small linear trend in the radial velocities (RVs) with the time. The latter obtained 9 spectra distributed over 2.8 years. The whole FEROS+HARPS spectroscopic ob-

servations cover a period of more than 9 years. We analyzed the RVs obtained with these spectrographs, correcting the values for the offset of 0.180 km/s obtained by de Medeiros et al. (2009). The result is shown in Fig. 4, where an orbital period of 11.4 years was found. A detailed discussion of the spectroscopic orbital parameters is far from the purpose of this work, where the RV data were used by us only to confirm the binarity of HD12438. Using a mass value for the primary component of $M_1 = 1.02 \pm 0.19 M_{\odot}$ (da Silva et al. 2006) and assuming a mass of the secondary of $M_2 \sim 0.5 M_{\odot}$ deduced from the flux ratio, the angular semi-major axis for a minimum orbital period of 11 years (at a distance of 52.8 pc, see Table 2) is > 70 mas. This means that the binary is highly inclined toward the line of sight. This also explains the small RV amplitude variations observed.

As previously mentioned, by fitting Eq. 5 we estimated the angular diameter of the primary component. This value is in agreement with the estimate by da Silva et al. (2006). The temperature of the primary was derived by combining the averaged UD angular diameter and the bolometric luminosity.

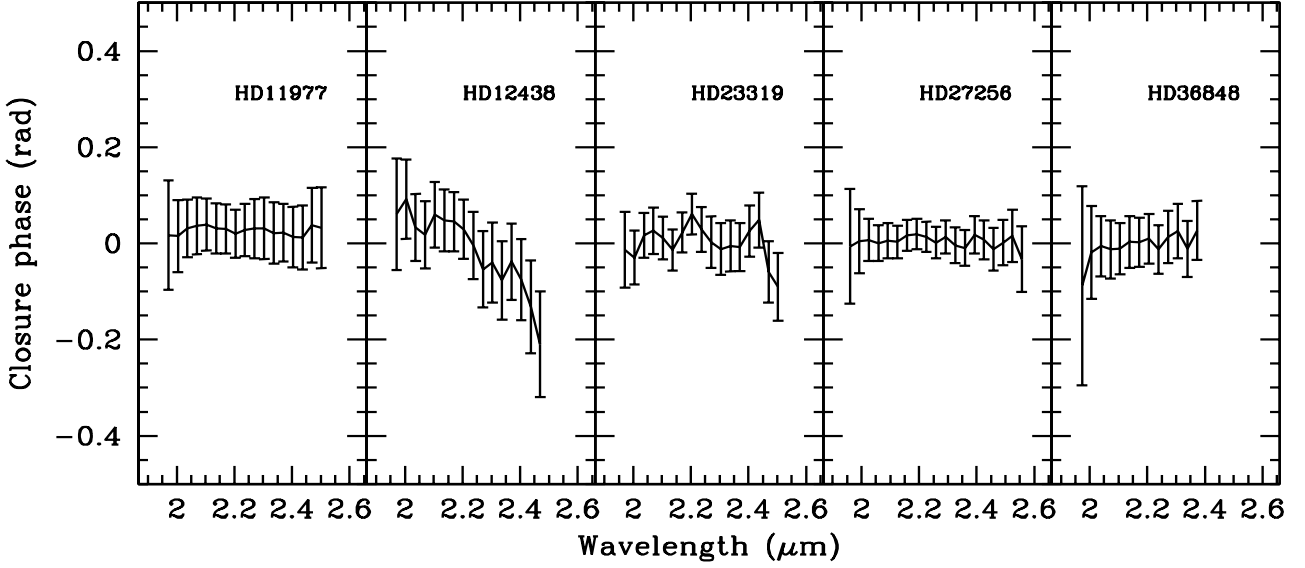


Fig. 3. Closure phase in the K band for the 5 giant stars observed with AMBER. HD12438, that we found to be a binary, has a closure phase different from zero for wavelengths $> 2.1 \mu\text{m}$. The other giant stars have closure phase close to zero, as expected.

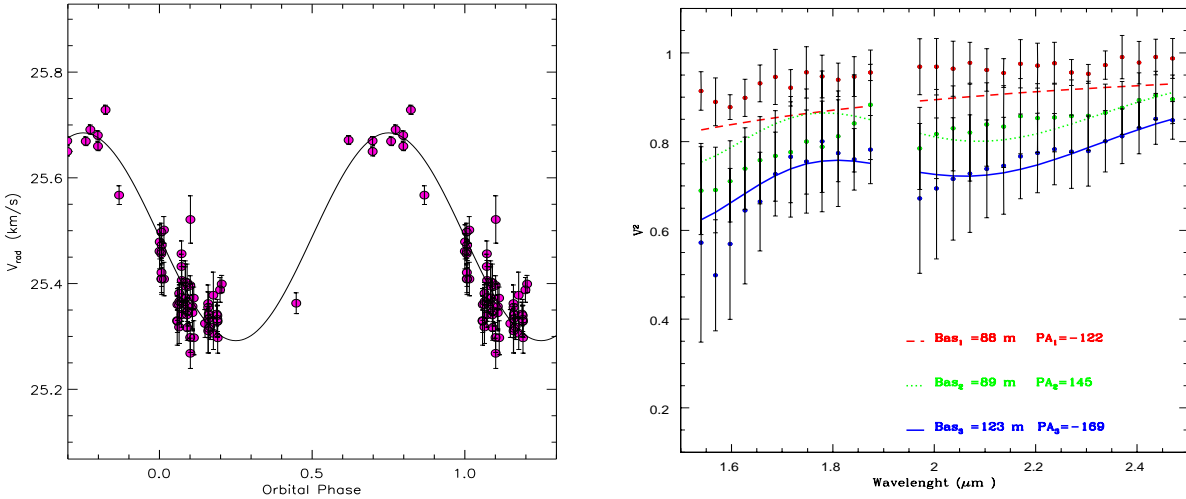


Fig. 4. *Left:* RV data of HD12438 obtained with FEROS and HARPS during more than 9 years. The line represent the orbit with lower rms obtained for a period of 11.4 years fixing the eccentricity to $e=0$. The high scatter around this line is mainly due to stellar oscillations. *Right:* Squared visibilities of HD12438 observed the 6th of October 2008. The lines are the visibilities of a binary (see Eq. 5), for the baselines of the observation, obtained with a separation of the components of ~ 12 mas and a position angle of 120° .

5. Discussion and conclusions

In this work we derived angular diameters of five field giant stars, selected from the sample of da Silva et al. (2006). In particular, using the AMBER@VLTI instrument combined with the fringe tracker FINITO, we were able to measure through UD and LD-fitting the angular diameters of HD23319 and HD27256 with accuracy of 3.2% and 4.1%, respectively when both the statistical and systematic error are taken into account. For HD11977 and HD36848 the relative error of the angular diameter was of 6.2% and 9.8%, respectively. The visibilities of

the giant star HD12438 were not reproducible by a single star model. We detected the companion star by interferometry, and we confirm and assess the period from radial velocity measurements. Fig. 5 shows the comparison between the LD angular diameters averaged overall the H and K bands and the predicted angular diameters derived by da Silva et al. (2006). The two set of values are consistent within 1.5σ . The difference between UD and LD diameters for our sample of stars is smaller than $< 0.8\%$, and in the case of HD11977 $\sim 0.15\%$.

Combining the LD angular diameters and the bolometric fluxes, we were able to derive the effective temperatures, which,

as shown in Fig. 5, are always lower than the values coming from spectroscopic analysis (see da Silva et al. 2006). This is interesting as far as the ongoing debate on metallicity of giant stars is concerned. The da Silva et al. (2006) data analysis is at the basis of the results which were used by Pasquini et al. (2007) to show that giants hosting planets are not preferentially metal rich, in contrast to the main sequence stars. One possibility to explain the discrepancy with main sequence stars is that metallicities of giant stars are systematically too low (see, e.g., Santos et al. 2008). In fact, the iron abundance depends on other parameters such as T_{eff} , $\log g$, and microturbulence. A higher T_{eff} corresponds to a higher $[\text{Fe}/\text{H}]$, if the $\log g$ and the microturbulent velocity are kept constant. Our LD interferometric results (LD-fitting) show lower temperatures for giant stars when compared to da Silva et al. (2006), and are indeed in the direction of a lower estimate of $[\text{Fe}/\text{H}]$, supporting the idea of Pasquini et al. (2007). Similar result was reported by Biazzo et al. (2007), which found on average a lower T_{eff} compared to da Silva et al. (2006).

The case of HD12438 points out that high inclined stellar binary systems which can be wrongly identified as planet hosting stars are not so rare. HD12438 shows that optical long baseline interferometry is a useful tool to detect such systems. The binarity of the system, in fact, can be only detected if the flux ratio between the primary star and the companion is much higher than typical value for star/planet.

Future high accurate spectroscopic time-series observations of these giant stars will allow to determine the masses by combining the asteroseismologic analysis with the interferometric diameter. In the case of HD12438 spectroscopic observation will also constrain the binary orbit.

Acknowledgements. We thank the anonymous referee for the useful comments and suggestions. This research has made use of the AMBER data reduction package of the Jean-Marie Mariotti Center⁴. C. Paladini acknowledge the support of the Project P19503-N16 of the Austrian Science Fund (FWF).

References

- Bedding, T. R., Huber, D., Stello, D., et al. 2010, *ApJ*, 713, L176
 Biazzo, K., Pasquini, L., Girardi, L., et al. 2007, *A&A*, 475, 981
 Bordé, P., Coudé du Foresto, V., Chagnon, G., & Perrin, G. 2002, *A&A*, 393, 183
 Cardelli, J. A., Clayton, G. C., & Mathis, J. S. 1989, *ApJ*, 345, 245
 Chelli, A., Utrera, O. H., & Duvert, G. 2009, *A&A*, 502, 705
 Claret, A., Diaz-Cordoves, J., & Gimenez, A. 1995, *A&AS*, 114, 247
 da Silva, L., Girardi, L., Pasquini, L., et al. 2006, *A&A*, 458, 609
 de Medeiros, J. R., Setiawan, J., Hatzes, A. P., et al. 2009, *A&A*, 504, 617
 Dyck, H. M., van Belle, G. T., & Thompson, R. R. 1998, *AJ*, 116, 981
 Efron, B. 1979, *The annals of Statistics*, 7, 1
 Endl, M., Cochran, W. D., Kürster, M., et al. 2006, *ApJ*, 649, 436
 Guenther, E. W., Hartmann, M., Esposito, M., et al. 2009, *A&A*, 507, 1659
 Haguenauser, P., Abuter, R., Alonso, J., et al. 2008, in Presented at the Society of Photo-Optical Instrumentation Engineers (SPIE) Conference, Vol. 7013, Society of Photo-Optical Instrumentation Engineers (SPIE) Conference Series
 Hanbury Brown, R., Davis, J., Lake, R. J. W., & Thompson, R. J. 1974, *MNRAS*, 167, 475
 Hartmann, M., Guenther, E. W., & Hatzes, A. P. 2010, *ApJ*, 717, 348
 Hatzes, A. P. & Zechmeister, M. 2007, *ApJ*, 670, L37
 Hekker, S., Kallinger, T., Baudin, F., et al. 2009, *A&A*, 506, 465
 Jacob, A. P. & Scholz, M. 2002, *MNRAS*, 336, 1377
 Johnson, J. A., Butler, R. P., Marcy, G. W., et al. 2007, *ApJ*, 670, 833
 Kallinger, T., Weiss, W. W., Barban, C., et al. 2010, *A&A*, 509, A77+
 Kennedy, G. M. & Kenyon, S. J. 2008, *ApJ*, 673, 502
 Kjeldsen, H. & Bedding, T. R. 1995, *A&A*, 293, 87
 Kornet, K., Wolf, S., & Różycka, M. 2006, *A&A*, 458, 661
 Le Bouquin, J.-B., Abuter, R., Bauvir, B., et al. 2008, in Presented at the Society of Photo-Optical Instrumentation Engineers (SPIE) Conference, Vol. 7013, Society of Photo-Optical Instrumentation Engineers (SPIE) Conference Series
 Mérand, A., Bordé, P., & Coudé du Foresto, V. 2005, *A&A*, 433, 1155
 North, J. R., Davis, J., Bedding, T. R., et al. 2007, *MNRAS*, 380, L80
 Paladini, C., Aringer, B., Hron, J., et al. 2009, *A&A*, 501, 1073
 Pasquini, L., Döllinger, M. P., Weiss, A., et al. 2007, *A&A*, 473, 979
 Petrov, R. G., Malbet, F., Weigelt, G., et al. 2007, *A&A*, 464, 1
 Pickles, A. J. 1998, *PASP*, 110, 863
 Raymond, S. N., Scalo, J., & Meadows, V. S. 2007, *ApJ*, 669, 606
 Santos, N. C., Melo, C., James, D. J., et al. 2008, *A&A*, 480, 889
 Setiawan, J., Pasquini, L., da Silva, L., et al. 2004, *A&A*, 421, 241
 Setiawan, J., Rodmann, J., da Silva, L., et al. 2005, *A&A*, 437, L31
 Skrutskie, M. F., Cutri, R. M., Stiening, R., et al. 2006, *AJ*, 131, 1163
 Tatulli, E., Millour, F., Chelli, A., et al. 2007, *A&A*, 464, 29
 van Leeuwen, F. 2007, *A&A*, 474, 653

⁴ Available at <http://www.jmmc.fr/amberdrs>

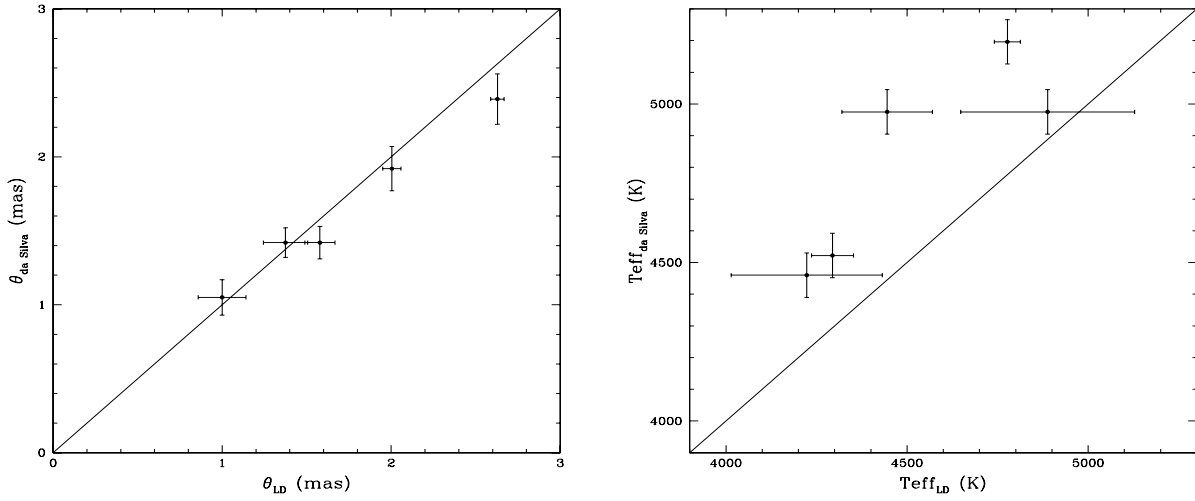


Fig. 5. *Left:* Comparison between interferometric-measured LD angular diameters and model precision by da Silva et al. (2006). The LD diameters were obtained averaging the LD diameters in the H and K bands. *Right:* Comparison between the effective temperatures obtained using the Eq.4 and the spectroscopic temperature derived by da Silva et al. (2006). The interferometric derived temperature are systematically lower than the spectroscopic ones.